minerals

MDPI

Article

Development of Low-Alkali, Fly Ash/Slag Geopolymers: Predictive Strength Modelling and Analyses of Impact of Curing Temperatures

Supphatuch Ukritnukun [1], Pramod Koshy [1,*], Clayton Feng [1], Aditya Rawal [2], Arnaud Castel [3,4] and Charles Christopher Sorrell [1]

[1] School of Materials Science and Engineering, UNSW Sydney, Sydney, NSW 2052, Australia; usupphatuch@gmail.com (S.U.); clayton.feng@student.unsw.edu.au (C.F.); c.sorrell@unsw.edu.au (C.C.S.)
[2] Mark Wainwright Analytical Centre, NMR Facility, UNSW Sydney, Sydney, NSW 2052, Australia; a.rawal@unsw.edu.au
[3] School of Civil and Environmental Engineering, UNSW Sydney, Sydney, NSW 2052, Australia; arnaud.castel@uts.edu.au
[4] School of Civil and Environmental Engineering, University of Technology, Ultimo, NSW 2007, Australia
* Correspondence: koshy@unsw.edu.au

Abstract: The present work analyses the effects of curing temperature (25, 40, 60 °C for 24 h), silicate modulus Ms value (1.5, 1.7, 2.0), and slag content (10, 20, 30, 40 wt%) on the compressive strength development (1, 7, 14, 28 days) of low-alkali geopolymer mortars with matrices from fly ash and blast furnace slag. These data were used to generate predictive models for 28-day compressive strength as a function of curing temperature and slag content. While the dominant variable for the 1-day compressive strength was the curing temperature, the slag content was dominant for the 28-day compressive strength. The ratio of the 1-day and 28-day compressive strengths as a function of curing temperature, *Ms* value, and slag content allows prediction of the maximal possible curing temperature and shows cold-weather casting to present an obstacle to setting. These data also allow prediction of the 28-day compressive strength using only the 1-day compressive strength.

Keywords: geopolymer; heat curing; strength prediction; fly ash; slag

Citation: Ukritnukun, S.; Koshy, P.; Feng, C.; Rawal, A.; Castel, A.; Sorrell, C.C. Development of Low-Alkali, Fly Ash/Slag Geopolymers: Predictive Strength Modelling and Analyses of Impact of Curing Temperatures. *Minerals* **2021**, *11*, 60. https://doi.org/10.3390/min11010060

Received: 26 November 2020
Accepted: 6 January 2021
Published: 11 January 2021

1. Introduction

Geopolymers are novel low CO_2 substitutes for ordinary Portland cement (OPC) [1] and are fabricated by reacting aluminosilicate- and/or silica-containing sources such as low-CaO Class F fly ash (FA), metakaolin (MK), and ground granulated blast furnace slag (GGBFS) with an alkaline activator solution. The activator solution is comprised of hydroxides or silicates of alkalis, with sodium hydroxide and sodium silicate being the most common [2]. The geopolymer structures can have a two- or three-dimensional aluminosilicate network, which consists of repeating units of $(Si\text{-}O\text{-}Al\text{-}O)_n$ and $(Si\text{-}O\text{-}Al\text{-}Si\text{-}O\text{-})_n$ [2]. The silicate modulus (Ms) is the mass ratio of the SiO_2/Na_2O amounts present in the activator solution [2]. This is an important consideration for standardisation of the activator composition when mixtures of sodium hydroxide (of varying molarities) and sodium silicate of varying Na_2O/SiO_2 molar ratios are used for the activation process. The silicate modulus can impact on the viscosity and subsequent reactivity of the activator solution as has been demonstrated in previous work [3].

Thermally-cured, low-calcium, fly-ash-based, geopolymer concretes have exhibited excellent mechanical strengths and durability in short-term and long-term tests [4–6]. The structural behaviour of reinforced columns [7], bond strength between geopolymer concrete and reinforcing bars [8], fracture properties [9], and creep/drying shrinkage [10] of these products have been found to be similar or superior to those of members of OPC concrete.

The curing temperature plays an important role in the dissolution of Si^{4+} and Al^{3+} from the source materials by the alkali activator solution [11]. Curing at elevated temperatures is done to overcome the activation energy for dissolution of the aluminosilicate glass of fly ash, the calcium-aluminosilicate glass of blast furnace slag, and the aluminosilicate pseudomorph metakaolin, in the alkali activator solution. The activation energy barriers are reported to be in the order fly ash (glass + mullite + quartz) > blast furnace slag (glass) > metakaolin (pseudocrystalline solid) owing to the relative degrees of crystallinity [12–14]. Leaching of Si^{4+} and Al^{3+} from fly ash at 80°C was observed to be significantly greater than that from blast furnace slag [11]. In contrast, room-temperature leaching showed a converse effect. These data suggest that sufficient solubilities and kinetics for practical geopolymerisation can be achieved at lower curing temperatures through the use of compositions rich in blast furnace slag.

One of the most informative studies is by Rovnaník [15], who investigated the effect of curing temperature on the setting behaviour and compressive strengths of metakaolin-based geopolymer mortars. These data, which are shown in Figure 1A, reveal the following trends:

- Curing and ageing continuously at 10 °C: Setting delay of >3 days, followed by linear strength development;
- Curing and ageing continuously at 20 °C: Logarithmic strength development;
- Curing at 40 °C, followed by ambient ageing: Strength maximisation by 3 days ageing;
- Curing at 60 or 80 °C for 4 h, followed by ambient ageing: Strength maximisation by 20 h ageing.

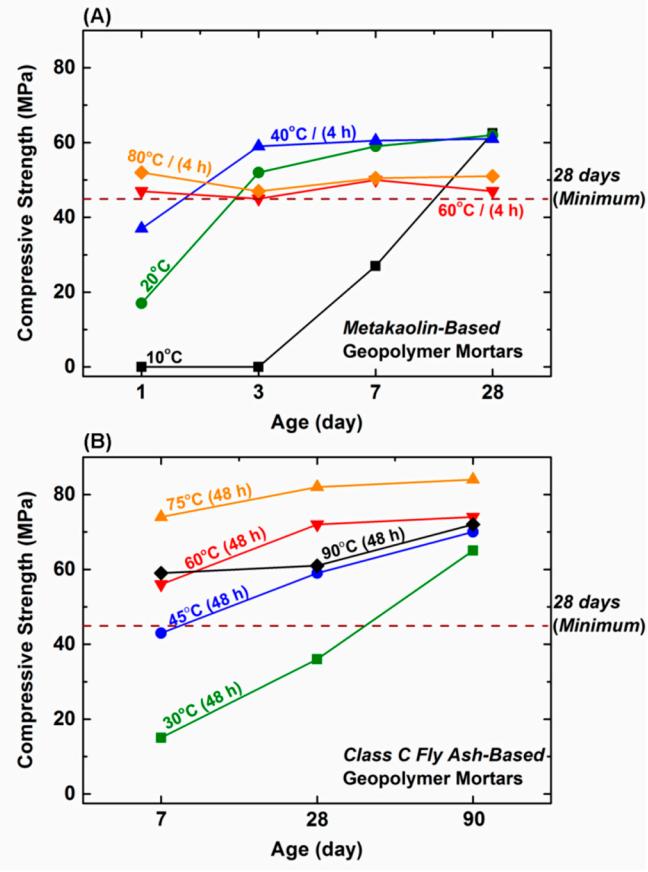

Figure 1. Compressive strength variation as a function of ageing under ambient conditions (~25 °C), following initial curing conditions (as indicated) of (**A**) metakaolin + sodium silicate based geopolymer mortars and (**B**) Class C fly ash + sodium silicate geopolymer mortars. Adapted from [15,16].

These curing conditions resulted in differential 28-day strengths in which the two highest curing temperatures exhibited lower strengths than those of the three lower curing temperatures. This differential could be correlated with a similar differential in the apparent porosities, which is likely to have resulted from the effects of water evaporation during curing.

In a second comprehensive study, Chindaprasirt et al. [16] investigated the compressive strengths of geopolymer mortars based on high-CaO Class C fly ash that were cured for 48 h at different temperatures, followed by ambient ageing to 90 days. As shown in Figure 1B, for curing between 30° and 75 °C, the compressive strength increased significantly with curing temperature as well as with ageing time, although the effect of the latter decreased with increasing curing temperature. The sole exception was for curing at 90 °C, which resulted in samples that generally were weaker than for curing at 75 or 60 °C. Again, this was attributed to evaporation of water during curing. Similar trends were observed for geopolymer concretes based on Class F ash by Noushini et al. [17].

In terms of the curing time, Figure 1A demonstrates that a curing time of 4 h is sufficient for setting as well as the achievement of the required 28-day compressive strength. More generally, curing typically is done for times in the range 4–24 h, where the longer times generate higher compressive strengths [6,15,17]. Comparison between Figure 1A,B suggest that the longer curing time of 48 h paradoxically may yield greater strengths at the higher curing temperatures.

Table 1 provides a comprehensive summary of studies on the processing and properties of geopolymer mortars based on fly ash + blast furnace slag fabricated by heat curing.

There has been work on curing of geopolymer concretes at high temperatures and with mixtures not containing fly ash and blast furnace slag [31–36]; however, since the focus is on geopolymer mortars, these have not been shown in the table.

As seen from Table 1, there has been a significant volume of work on the effects of heat curing of geopolymers comprised of fly ash and/or slag on the compressive strength. However, there has not been any systematic investigation of the simultaneous effects of curing temperatures (25, 40, 60 °C for 24 h), silicate modulus Ms values (1.5, 1.7, 2.0), and fly ash/slag ratios (90/10, 80/20, 70/30, 60/40 wt%) on the compressive strength development (1, 7, 14, 28 days) for geopolymer mortars. Further, there do not appear to be any studies that have attempted to model the effects of any of these variables on the compressive strengths. Consequently, these are the foci of the present.

Table 1. Comprehensive summary of geopolymer mortars cured at high temperatures ([1] Percentages are wt%; [2] Some compressive strength values have been approximated from the graphical representations; [3] A:L:S = Aluminosilicate (fly ash + slag): Liquid alkaline activator (Na_2SiO_3 + NaOH): Sand ratio by mass; [4] w/b = water/binder ratio by mass; [5] Final silicate modulus (Ms) was calculated from mass ratio given in the study; [6] Age at 2 days; [7] Age at 7 days).

Aluminosilicate Source [1]		Alkaline Activator Proportions			Proportion		Specimen Shape & Size		Curing Conditions			Compressive Strength (MPa)[2]		Ref.
Fly Ash	Slag	Components	Mix		A:L:S [3]	w/b [4]	Shape	Size (mm)	Temp (°C)/Time (h)		Type	Age (days)		
		Na_2SiO_3	NaOH	Silicate Modulus [5]								1	28	
Coarse 100%	0%	Ms = 2.22	10 M	Ms = 0.84	1:0.5:2.75	0.05	Cube	50 × 50 × 50	75	48	Air-tight	N/A	38	[16]
Medium 100%													53	
Fine 100%													75	
100%	0%	Ms = 3.44	5 M	Ms = 1.60	1:0.7:2	N/A	Cylinder	ϕ = 25 H = 25	65	48	Oven-cured	24 [6]	N/A	[18]
			10 M	Ms = 1.05								35 [6]		
			15 M	Ms = 0.78								33 [6]		
100%	0%	Ms = 2.16	13.11 M	Ms = 0.72	1:0.4:3	0.3	Cube	71 × 71 × 71	60	24	Oven-cured	56	N/A	[19]
									90	24		56.5		
									120	24		58		
100%	0%	Ms = 2.04	N/A	Ms = 1.0	1:0.2:2.75	0.5	Cube	50 × 50 × 50	25	672	Air-tight	N/A	20	[20]
50%	50%												89	
0%	100%												62	
100%	0%	Ms = 2.70	8 M	Ms = 1.57	1:0.46:1	0.45	Cube	100 × 100 × 100	60	24	Oven-cured	N/A	52	[21]
90%	10%												54	
80%	20%												55	
70%	30%												56	
60%	40%												58	
50%	50%												59	
40%	60%												62	
30%	70%												65	
20%	80%												72	
10%	90%												77	
0%	100%												82	

Table 1. *Cont.*

Aluminosilicate Source [1]		Alkaline Activator Proportions			Proportion		Specimen Shape & Size		Curing Conditions			Compressive Strength (MPa)[2]		Ref.
Fly Ash	Slag	Components	Mix		A:L:S [3]	w/b [4]	Shape	Size (mm)	Temp (°C)/Time (h)		Type	Age (days)		
		Na_2SiO_3	NaOH	Silicate Modulus [5]								1	28	
100%	0%	Ms = 2.70	12 M	Ms = 1.32	1:0.46:1	0.45	Cube	100 × 100 × 100	60	24	Oven-cured	N/A	53	
90%	10%												55	
80%	20%												57	
70%	30%												59	
60%	40%												61	
50%	50%												65	
40%	60%												68	
30%	70%												74	
20%	80%												77	
10%	90%												82	
0%	100%												85	
100%	0%	Ms = 2.70	16 M	Ms = 1.14	1:0.46:1	0.45	Cube	100 × 100 × 100	60	24	Oven-cured	N/A	54	
90%	10%												58	
80%	20%												62	
70%	30%												63	
60%	40%												65	
50%	50%												66	
40%	60%												69	
30%	70%												73	
20%	80%												78	
10%	90%												83	
0%	100%												87	

Table 1. *Cont.*

Aluminosilicate Source [1]		Alkaline Activator Proportions			Proportion		Specimen Shape & Size		Curing Conditions			Compressive Strength (MPa)[2]		Ref.
Fly Ash	Slag	Components	Mix		A:L:S [3]	w/b [4]	Shape	Size (mm)	Temp (°C)/Time (h)		Type	Age (days)		
		Na_2SiO_3	NaOH	Silicate Modulus [5]								1	28	
100%	0%	Ms = 2.39	6 M	Ms = 1.52	1:0.6:1	N/A	Cube	50 × 50 × 50	25	N/A	Air-tight	N/A	38.5	[22]
			10 M	Ms = 1.25									50.5	
			14 M	Ms = 1.06									56.0	
100%	0%	Ms = 2.07	14 M	Ms = 1.06	1:0.35:0.6	N/A	Cylinder	ϕ = 25 H = 50	70	24	Oven-cured	57 [7]	N/A	[23]
100%	0%	Ms = 2.22	10 M	Ms = 0.64	N/A	0.4	Cube	50 × 50 × 50	23	24	Oven-cured	N/A	57	[24]
									40	24				
100%	0%	Ms = 2.41	10 M	Ms = 1.08	1:0.6:2.75	0.6	Cube	50 × 50 × 50	23	24	Oven-cured	N/A	50	[25]
									75	24				
100%	0%	Ms = 2.17	10 M	Ms = 0.51	1:0.55:2.75	0.35	Cube	50 × 50 × 50	80	4	Oven-cured	N/A	11	[26]
										6			12	
										20			19	
									100	4			13	
										6			18	
										20			22	
									120	4			14	
										6			19	
										20			33	
									25	672	Air-tight		15	
100%	0%	N/A	5 M	N/A	N/A	N/A	Cylinder	ϕ = 25 H = 25	65	48	Oven-cured	48	N/A	[27]
			10 M									65		
			15 M									58		

Table 1. *Cont.*

Aluminosilicate Source [1]		Alkaline Activator Proportions			Proportion		Specimen Shape & Size		Curing Conditions			Compressive Strength (MPa)[2]		Ref.
Fly Ash	Slag	Components	Mix		A:L:S [3]	w/b [4]	Shape	Size (mm)	Temp (°C)/Time (h)		Type	Age (days)		
		Na_2SiO_3	NaOH	Silicate Modulus [5]								1	28	
100%	0%	Ms = 2.22	10 M	Ms = 0.64	1:0.5:2.75	0.05	Cube	50 × 50 × 50	30	24	Oven-cured	8	N/A	[28]
									45	24		20		
									60	24		37		
									75	24		50		
									90	24		25		
			10 M	0.64	1:0.5:2.75	0.05			25 75	1 72		48		
				0.84								55		
				1.06								47		
				1.43								40		
			15 M	0.48	1:0.5:2.75	0.05			25 75	1 72		65		
				0.65								57		
				0.85								31		
				1.23								42		
			20 M	0.38	1:0.5:2.75	0.05			25 75	1 72		51		
				0.53								62		
				0.71								38		
				1.07								50		
100%	0%	Ms = 2.0	10 M	1.00	1:0.55:1.25	0.5	Cylinder	50 × 100	70	24	Oven-cured	N/A	8.10^7	[29]
80%	20%	Ms = 2.0	10 M	1.00	1:0.55:1.25	0.5	Cylinder	50 × 100	70	24	Oven-cured	N/A	26.5^7	
60%	40%	Ms = 2.0	10 M	1.00	1:0.55:1.25	0.5	Cylinder	50 × 100	70	24	Oven-cured	N/A	34.1^7	
0%	100%	Ms = 3.49	14 M	0.94	1:1:3	N/A	Prism	40 × 40 × 160	60	24	Oven cured	N/A	21.5^7	[30]
25%	75					N/A						N/A	13.5^7	
50%	50					N/A						N/A	12.5^7	
75%	25					N/A						N/A	11.5^7	

2. Experimental

2.1. Materials

The Class F fly ash was obtained from the Eraring Power Station, NSW, Australia while the ground granulated blast furnace slag was obtained from Blue Circle Southern Cement Limited, Sydney, NSW, Australia. These materials comply with requirements stated in AS 3582.1 [37] and AS 3582.2 [38], respectively. The chemical compositions of the samples are shown in Table 2.

Table 2. Chemical compositions of raw materials.

Oxide	Fly Ash (wt%)	Slag (wt%)
SiO_2	64.63	33.84
Al_2O_3	24.40	13.76
Na_2O	0.73	0.38
K_2O	2.31	0.28
CaO	1.68	41.75
MgO	0.63	5.59
Fe_2O_3	2.91	0.56
SO_3	0.14	2.42
Loss on Ignition (LOI)	1.34	0.13
Total	98.77	98.71

X-ray diffraction analysis was conducted using a PANalytical X'pert (Malvern PANalytical, Sydney, Australia) MPD (Multi-Purpose X-ray Diffraction System, 40 mA, 45 kV, CuKα radiation, 10–70° 2-theta range, 0.026° 2-theta min^{-1} scan speed). The pattern for the fly ash given elsewhere [3] showed the presence of quartz and mullite as the major crystalline phases while an aluminosilicate glass was the major phase present. The XRD pattern for the blast furnace slag was predominantly amorphous and this represents a calcium aluminosilicate glass [3]. Particle size measurements showed that the mean particle size of fly ash was 16.4 μm and that of slag was 13.3 μm. Mixtures of sodium hydroxide (NaOH) and sodium silicate solution were used for the activator process and the sources were NaOH pellets (98% purity, Ajax FineChem, Univar A-302) and sodium silicate solution (Grade D, PQ Australia) with a composition of SiO_2 = 29.4 wt%, Na_2O = 14.7 wt%, and H_2O = 55.9 wt% and Ms = 2.0. These solutions were mixed and homogenised for 24 h prior to casting to produce activator solutions of Ms = 1.5, 1.7, and 2.0. The fine aggregate used was washed beach sand (BC Sands, true density 2650 $kg{\cdot}m^{-3}$, water absorption 3.5%), both determined according to ASTM C128-15 [39]. After washing for 5 min, the sand was oven dried at 105 °C for 48 h and then prepared to a saturated surface dry (SSD) state prior to batching by adding 3.5 wt% water [40].

2.2. Mix Design

The geopolymer binder mass is the total amount of supplementary cementitious materials SCMs (fly ash and blast furnace slag), NaOH, and the SiO_2 and Na_2O in the sodium silicate. The mass of water is the sum of the masses of that in the sodium silicate solution and that of free water used to standardise the mixes. The typical water/binder mass ratios used for geopolymer mortars have been seen to range from 0.3 to 0.7 [13] and so a minimal value of 0.3 was selected to ensure sufficient workability while maintaining low apparent porosity. Data in the literature for geopolymer compositions [41–44] have shown that the strengths are generally highest for a mass ratio of activator to geopolymer binder in the range of 0.5–0.7, and thus for minimising the cost, the value of 0.5 was selected. Work in the literature has shown that the strength does not change significantly if the sand-to-geopolymer binder ratio is varied in the range of 0.5 to 1.5 [45] while the workability becomes difficult when the ratio exceeds 1.5, and the strength is lowered at values of 2.0–3.0 [23]. In the present work, the value of 1.5 was selected as a constant value

for the different mix proportions shown in Table 3. This ratio has been trialled previously and used for the determination of the ambient cured strengths [3].

Table 3. Geopolymer mortar mix proportions (g).

Mix No [1]	FA/S [2]	Fly Ash	Slag	Na_2SiO_3	NaOH	Sand [3]	Free Water
Ms = 2.0							
1	90/10	641.4	71.3	356.3	0.0	1069.0	62.0
2	80/20	570.1	142.5	356.3	0.0	1069.0	62.0
3	70/30	498.9	213.8	356.3	0.0	1069.0	62.0
4	60/40	427.6	285.1	356.3	0.0	1069.0	62.0
5	50/50	356.3	356.3	356.3	0.0	1069.0	62.0
6	40/60	285.1	427.6	356.3	0.0	1069.0	62.0
Ms = 1.7							
7	90/10	638.4	70.9	340.9	13.8	1064.0	72.0
8	80/20	567.5	141.9	340.9	13.8	1064.0	72.0
9	70/30	496.5	212.8	340.9	13.8	1064.0	72.0
10	60/40	425.6	283.7	340.9	13.8	1064.0	72.0
11	50/50	354.7	354.7	340.9	13.8	1064.0	72.0
12	40/60	283.7	425.6	340.9	13.8	1064.0	72.0
Ms = 1.5							
13	90/10	636	70.7	330.2	23.1	1060.0	80.0
14	80/20	565.3	141.3	330.2	23.1	1060.0	80.0
15	70/30	494.7	212.0	330.2	23.1	1060.0	80.0
16	60/40	424.0	282.7	330.2	23.1	1060.0	80.0
17	50/50	353.3	353.3	330.2	23.1	1060.0	80.0
18	40/60	282.7	424.0	330.2	23.1	1060.0	80.0

[1] Mix proportions were designed to ensure a final unit weight of 2200 g, [2] FA/S = Fly ash/Slag mass ratio, [3] Sand in the SSD condition.

In effect, the experimental design was based on the modelling of the compressive strength development in terms of the controllable variables fly ash/slag ratio, Ms ratio, and curing temperature while minimising the effects of the uncontrollable variables that develop during curing, such as cracking from shrinkage and pore formation from water evaporation.

The mortars were prepared by firstly mixing fly ash and blast furnace slag in a 5 L Hobart mixer for 3 min, after which the alkaline activator solution was added and mixing was continued for an additional 5 min to activate the raw materials. Then sand was added and mixing was continued for an additional 5 min. Then the blended mix was transferred to a mould and spread into sixteen individual cavities. The moulds were then filled by vibratory casting on a vibrating table for 3 min and, if the filling was not sufficient, additional material was used to supplement it. Excess material was then removed by scraping using a guillotine. After the casting was done, the mould was placed in a zip-lock plastic bag and sealed. Curing was then done at temperatures of 25, 40, or 60°C for 24 h. The cured was done in an oven to ensure consistent temperatures for the samples. After curing, the samples were removed from the mould and placed in an air-tight plastic container containing additional water to provide a hydrated atmosphere for the curing process until the time for testing.

2.3. Compressive Strength

The models developed in the present work are based on compressive strength development. Hence, the strengths were determined by uniaxial testing of the geopolymer mortar cubes (25 × 25 × 25 mm) using an Instron 5982 (Instron, Norwood, MA, USA) universal testing machine (loading rate of 1200 $N \cdot s^{-1}$). The cube size was chosen to ensure that the samples could be tested within the loading capability of the instrument (100 kN).

The testing was done based on ASTM C109-13 [46] and four samples were tested for each composition for each time point of 1, 7, 14, and 28 days of ageing.

3. Results and Discussion

3.1. Trends in Compressive Strength

Figure 2A–I show the effects of ageing (in days) on the compressive strength development of geopolymer mortars as a function of curing temperature (for 24 h), Ms value, and slag content while Figure 3 shows the minimal time required for samples to reach the 28-day compressive strength. The key observations are as follows:

- An increase in curing temperature resulted in the acceleration of the polymerisation reaction during curing for 24 h, although there was a decrease in the rate of strength development with increasing temperature for all Ms values.
- Curing at 60 °C achieved maximal compressive strength after 24 h of curing, although ageing effectively resulted in no further strength increase.
- A slag content of 10 wt% failed to meet the minimal 28-day strength requirement (45 MPa) at all curing temperatures and Ms values. Therefore, a minimum of 20 wt% slag is necessary for the fabrication of low-alkali heat-cured geopolymers.
- The mechanisms of strength development at all ageing times can be divided into two separate trends based on the relative slag proportions: low slag contents ($\leq$30 wt% slag) and high slag contents (>30 wt% slag). This effect is evidence for a mechanistic change between these compositional regimes [3].
- As shown in Figure 3, heat curing is beneficial owing to the reduction in the ageing time required for geopolymer mortars to achieve the minimal 28-day strength requirement. However, the curing temperature, slag content, and Ms value are linked in that geopolymer mortars are more likely to fail to reach this strength requirement with increasing curing temperature at Ms = 2.0.
- Figure 3 also showed that lower Ms values accelerate the kinetics during the first 24 h, thus enabling the achievement of the required compressive strength in shorter times.
- In contrast, the effect of curing temperature and Ms value is not as apparent. That is, at Ms = 1.5, the kinetics are enhanced with increasing curing temperature while the trends at the other Ms values are inconsistent.
- These data also show that there is effectively no effect from the Ms value or slag content for the geopolymers that meet the 28-day strength requirement following curing at 60 °C. For the geopolymers that do meet this strength requirement following curing at 40 and 25 °C, decreasing the Ms value and increasing the slag content accelerated the kinetics of the reactions. These observations provide evidence for a mechanistic change between these temperature regimes over the ageing period.

3.2. Compressive Strength Factors

There are significant differences between the 1-day compressive strengths of ambient and heat-cured geopolymer mortars, as shown in Figure 4A–C. These data suggest that, even in this short time frame, the different mechanistic effects of composition are apparent (based on strength level and strength development trend differentials) while those of temperature are less obvious in that the highest slag content appears to show a logarithmic trend while the three lower slag contents appear to show largely linear or slightly exponential trends. The short time frame may have caused these effects to have insufficient time to be manifested clearly.

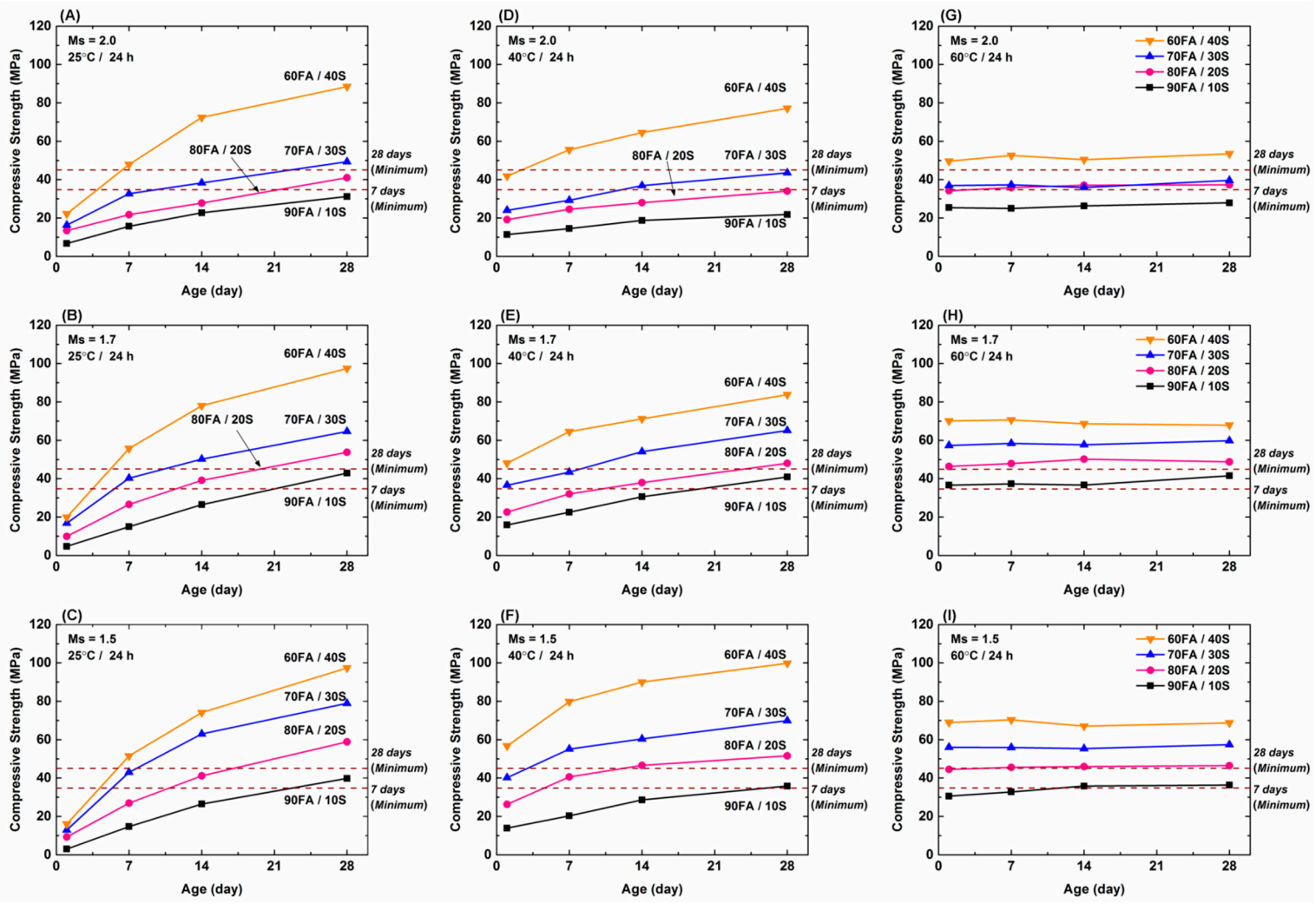

Figure 2. Effect of ageing on compressive strength development in geopolymer mortars as a function of temperature, Ms, and slag content. (**A**) Ms 2.0, Cured at 25 °C / 24 h, (**B**) Ms 1.7, Cured at 25 °C/24 h, (**C**) Ms 1.5, Cured at 25 °C/24 h, (**D**) Ms 2.0, Cured at 40 °C/24 h, (**E**) Ms 1.7, Cured at 40 °C/24 h, (**F**) Ms 1.5, Cured at 40 °C/24 h, (**G**) Ms 2.0, Cured at 60 °C/24 h, (**H**) Ms 1.7, Cured at 60 °C/24 h, (**I**) Ms 1.5, Cured at 60 °C/24 h.

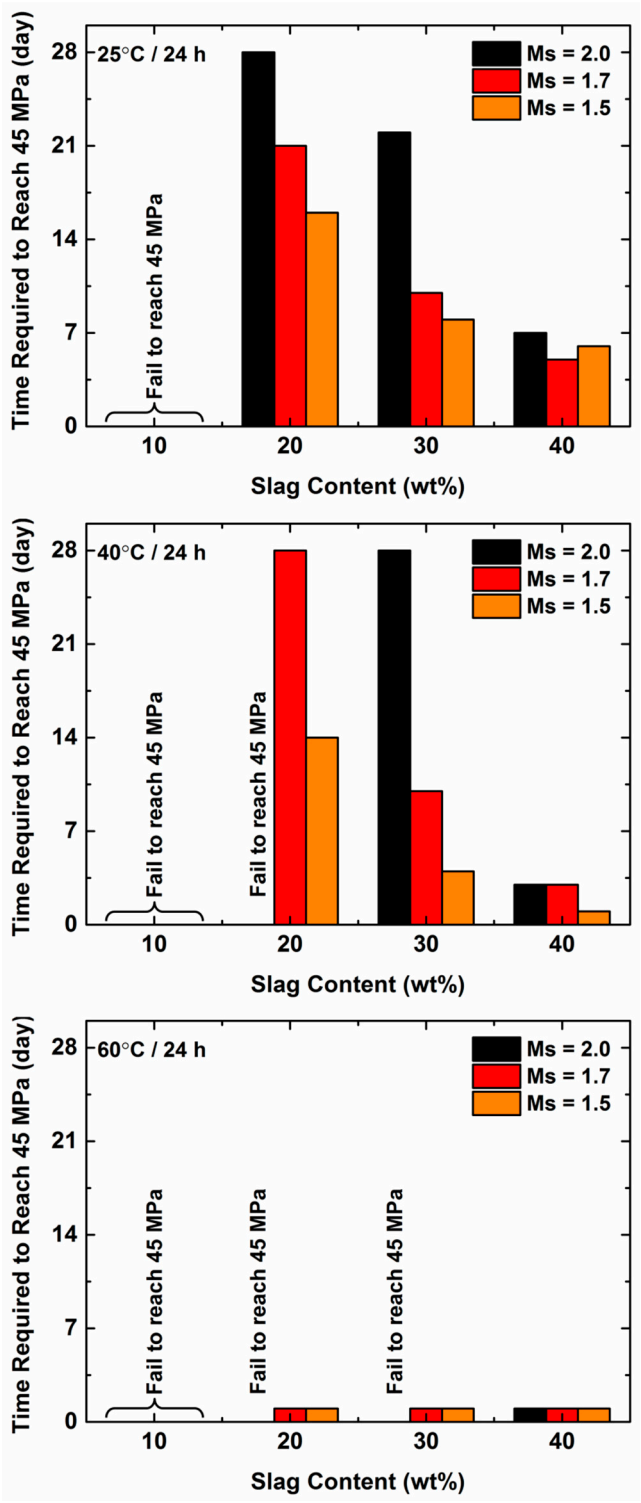

Figure 3. Minimal time required for samples to reach the 28-day compressive strength requirement of AS 3972 [47].

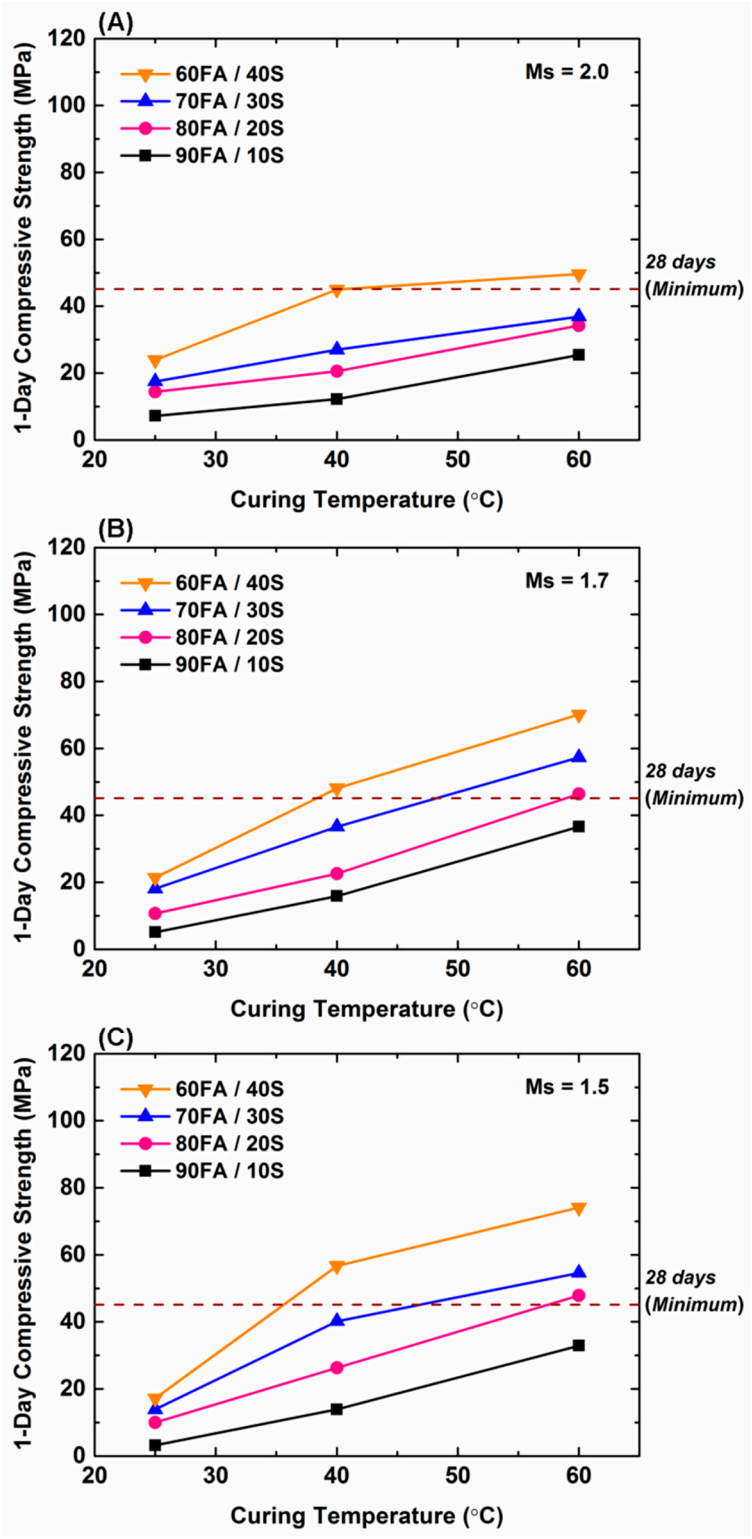

Figure 4. (**A**–**C**) 1-day compressive strength as a function of curing temperature, Ms value, and slag content.

Figure 5A,B summarises these data in terms of compressive strength factors, in which the strength of a heat-cured geopolymer mortar ($\sigma_{c,T}$) is divided by the strength of the corresponding ambient-cured geopolymer mortar ($\sigma_{c,25}$) for both the 1-day (incremental) and 28-day (decremental) ratios, respectively.

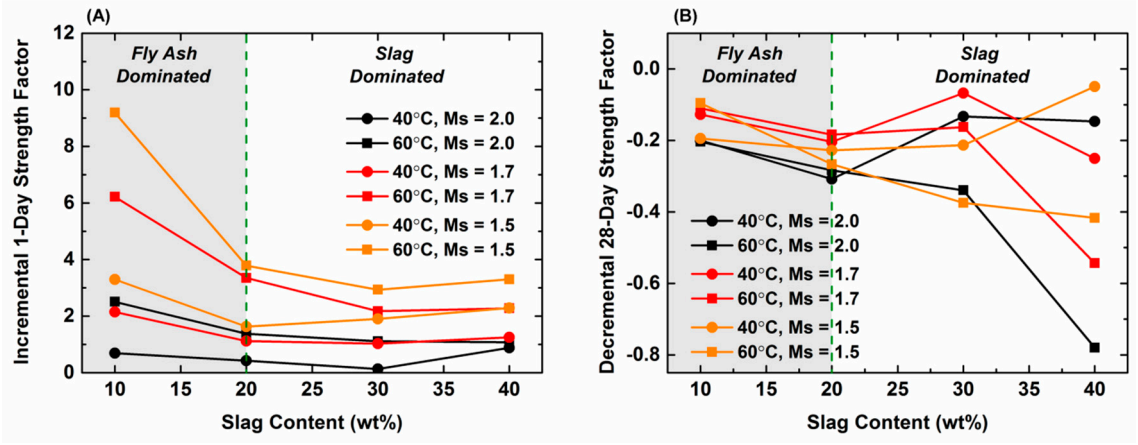

Figure 5. (**A**) Incremental strength factor (1-day compressive strength relative to that following curing at 25 °C for 24 h) (**B**) Decremental strength factor (28-day compressive strength relative to that following curing at 25 °C for 24 h) as a function of curing temperature, Ms value, and slag content.

3.2.1. 1-Day Incremental

These data indicate that geopolymer mortars cured at 40 °C show improvement in 1-day compressive strengths by incremental strength factors of 0.13–3.29, whereas samples cured at 60 °C exhibit more significant increases in the range 1.08–9.19, depending on the Ms value and slag content. Heat curing shows the greatest effect for the lowest slag content (10 wt% slag) although none of the geopolymer mortars achieved the 28-day compressive strength requirement. For the lower range of slag contents (10–20 wt%), the relative effects of the three variables can be differentiated, where:

For low slag content/Ms = 2.0, 1.7, 1.5:

Curing Temperature > Slag Content > Ms Value

For the range of higher slag contents (20–40 wt%), there is little effect of the slag content and the curing temperature, and Ms value has only a minor effect. These observations reflect the importance of the temperature on the leaching of Si^{4+} and Al^{3+} from fly ash during the early stage of geopolymerisation [16,17,23]. This explains why heat curing generally is done at low slag contents and Ms values < 1.5.

3.2.2. 28-Day Decremental

These data indicate that, for the lower range of slag contents (10–20 wt%), there is a slight decrease in the compressive strength factor at all curing temperatures and Ms values. However, at the higher range of slag contents (20–40 wt%), the trend is not as clear, where the data spread progressively with increasing slag content such that the overall behaviour falls into two categories for the effects of the variables:

For high slag content/Ms = 2.0:

Curing Temperature > Slag Content > Ms Value

For high slag content/Ms = 1.7, 1.5:

Slag Content > Curing Temperature > Ms Value

As mentioned earlier, this suggests the existence of two trends in behaviour as a function of low and high slag contents, which reflects different mechanisms for the two compositional regimes with 28 days ageing time [3]. While Figure 5A also suggests the existence of differential mechanisms between the 1-day compressive strength factors for 40

and 60°C, Figure 5B is more distinct in demonstrating this difference. Thus, these data also reflect different mechanisms between two temperature regimes [3].

3.3. Predictive Model for 28-Day Compressive Strength

Figure 6A–C shows the effect of curing temperature on the 28-day compressive strength as a function of Ms value and slag content. Unlike in the case of 1-day compressive strength, the 28-day compressive strengths (solid lines) decrease approximately linearly with increasing curing temperature for all Ms values. Increased curing temperature would be expected to enhance the dissolution of the fly ash in the activator solution, thereby increasing the compressive strength by enhancing gel formation after 1 day of curing relative to that at room temperature. However, heat curing would increase water evaporation from the gel structure as well as increase the viscosity of the silicate activator. These would reduce both the rate and extent of further reaction between the activator and the raw materials and the corresponding compressive strength development. Further, the slag reactivity would be enhanced with increased curing temperature, which would accelerate the setting and thus potentially result in rapid shrinkage and cracking of the samples, again decreasing the strength development. Hence, this procedural strategy addresses strength maximisation rather than setting time minimisation.

Table 4. Master equations for prediction of 28-day compressive strength (σ_{28}) as a function of curing temperature and slag content for different Ms values.

Ms	Low Slag Content (10, 20, 30 wt%)	High Slag Content (40 wt%)
2.0	Equation (1) $\sigma_{28} = (-0.0131 \times \text{Slag} \times T) + (-0.0174 \times T) + (1.42 \times \text{Slag}) + 21.10$	Equation (2) $\sigma_{28} = (-0.0713 \times \text{Slag} \times T) + (1.7275 \times T) + (5.562 \times \text{Slag}) - 103.91$
1.7	Equation (3) $\sigma_{28} = (-0.0113 \times \text{Slag} \times T) + (-0.0090 \times T) + (1.41 \times \text{Slag}) + 29.55$	Equation (4) $\sigma_{28} = (-0.0713 \times \text{Slag} \times T) + (1.8831 \times T) + (4.899 \times \text{Slag}) - 76.05$
1.5	Equation (5) $\sigma_{28} = (-0.0244 \times \text{Slag} \times T) + (0.1352 \times T) + (2.23 \times \text{Slag}) + 23.79$	Equation (6) $\sigma_{28} = (-0.0236 \times \text{Slag} \times T) + (0.107 \times T) + (2.9072 \times \text{Slag}) + 4.95$

For all curing temperatures and Ms values, the compressive strength increases with increasing slag content. Further, the rate of strength decrease as function of curing temperature increases with increasing slag content. Increasing the Ms value decreased the 28-day compressive strength, where the change between Ms = 1.5 and Ms = 1.7 is small but that between Ms = 1.7 and Ms = 2.0 is more significant. More generally, these data show that the effects of curing temperature and Ms value are fairly consistent, so there is no indication of the mechanistic change in terms of temperature regimes. However, the effect of slag content clearly can be differentiated between the highest and the three lower levels, again suggesting different mechanisms for two compositional regimes [3].

The apparent inconsistency in the absence of the indication of a change in reaction mechanism in terms of a temperature regime, while there is apparent consistency for a compositional regime, allows clarification of the roles of these two variables. Figures 2 and 4, Figures 5 and 6 show that the compositional effect is present at all ageing times. Figures 3 and 4, which highlight the effects of curing, show that the temperature effect can be observed during the curing period. Figure 6, which shows data for the 28-day compressive strength, do not indicate an effect of temperature. In effect, the temperature effect is expressed largely during the curing period. Therefore, in summary, the mechanistic change in terms of a compositional regime takes place during the ageing period while the mechanistic change of a temperature regime occurs only during the curing period.

The data in Figure 6 were used to extrapolate the 28-day compressive strength as a function of curing temperature (dotted lines). The differences between the highest slag content (high slag content) and the three lower slag contents (low slag content) are clear, again emphasising a change in reaction mechanism as a function of composition.

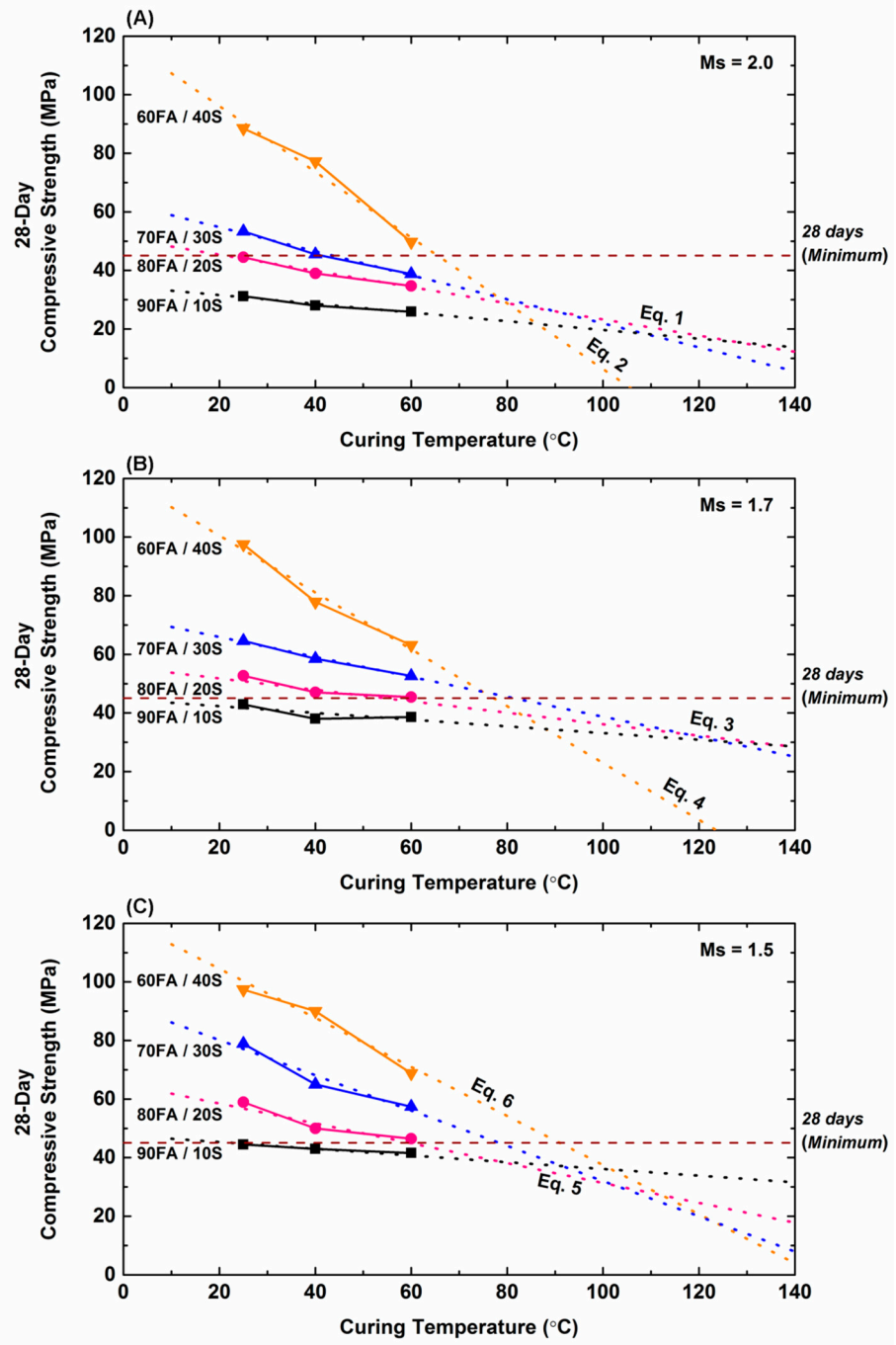

Figure 6. 28-day compressive strength (solid lines) and extrapolated values (dotted lines) as a function of curing temperature, slag content, and Ms (alkaline activator/SCM mass ratio = 0.5, water/binder ratio = 0.3) (Equations (Eq.) for these lines are shown in Table 4) (**A**) Ms 2.0, (**B**) Ms 1.7, (**C**) Ms 1.5.

These linear extrapolations were used to generate a model to (i) predict the 28-day compressive strength of geopolymer mortars cured outside the range of temperatures investigated and (ii) estimate the maximal curing temperature above which a 28-day compressive strength $\geq$45 MPa will not be reached. The data for high slag content were used directly to generate a master quadratic equation incorporating the curing temperature and slag content set at different Ms values; the three sets of data for low slag contents similarly were fit to another master equation. The resultant six master equations are given in Table 4. The plots shown in Figure 6 are based on the temperature range 25–60 °C because the H_2O vapour pressure as a function of temperature (~0.05–0.20 kPa) is approximately

exponential [48], doubling for each temperature and more than doubling again at 80 °C (~50 kPa). Hence, the range was limited so that water evaporation and associated compressive strength were minimised. The suitability of this strategy is indicated by coefficient of determination (R^2) values for the predictive equations, which were determined on the basis of linear fits to be in the range 0.90–0.97 for the six predictive equations shown in Figure 6 and Table 4. Thus, linear dependencies were concluded.

Comparison of the experimental data at reduced curing temperature for metakaolin-based geopolymer mortars (i.e., no slag, 4 h curing time) [15], shown in Figure 1A, with those for the lowest slag content in Figure 6 (i.e., nearly no slag, 24 h curing time), suggests that the two sets of data are consistent in that reduction of the curing temperature from ambient to 10 °C causes little or no change in the 28-day compressive strength. The investigator interpreted the results in terms of lower apparent porosities of the samples cured at 10 °C relative to those cured at ambient and higher temperatures. This conclusion was supported by the observation that the higher curing temperatures of 40, 60, and 80 °C correlated with increasing apparent porosities owing to the rapid evaporation of water during the heat curing for 4 h. Further, the empirical data supported the conclusion that there is a change in reaction mechanism between curing temperatures between 40 and 60 °C.

Comparison of the experimental data at increased curing temperatures for pure Class C fly ash-based geopolymer mortars (i.e., no slag, 48 h curing time) [16], shown in Figure 1B, with those for the lowest slag content in Figure 6 for blends of Class F fly ash and blast furnace slag (i.e., 10–40 wt% slag, 24 h curing time) demonstrate converse trends. That is, the pure fly ash mortars show increasing 28-day compressive strength with increasing curing temperature in the range 60–90 °C while the predicted strengths decrease. Further, a study of geopolymer concretes fabricated from 70 wt% Class F fly ash, 20 wt% *Kaolite High Performance Ash* (*HPA*), and 10 wt% slag [49] also revealed increasing 28-day compressive strength with increasing curing temperature. Both empirical studies revealed a mechanistic change at a temperature between 75 and 90 °C.

The key differentiating feature between these two empirical studies and the present work is that the former involved Ms values in the range 0.96–1.4 while the latter involved Ms values in the range 1.5–2.0. Examination of Figure 2A demonstrates that a combination of high curing temperature and low Ms value results in significant strength increase whereas Figure 6 shows a slight strength decrease. Consequently, these converse results are largely a result of the differences in Ms values at temperatures of ambient and above.

Owing to the clear importance of the Ms value, further refinement of the relationship between the curing temperature and the Ms value was done. Since the geopolymer mortars of the lowest slag content (10 wt%) consistently failed to achieve the 28-day compressive strength requirement, the data for the three higher slag contents from Figure 6 (using the intersections of the extrapolations and the 28-day (minimum) dashed line) were employed to generate generic equations incorporating the Ms values and the maximal curing temperatures (T_{Max}) to achieve the 28-day compressive strength requirement for different slag contents. Linear algebra was used to fit the data, whence it was found to match an elliptical trend and is defined by the equation:

$$ax^2 + bxy + cy^2 + dx + ey + f = 0 \quad (1)$$

where a–f are constants, x is the abscissa (Ms value), and y is the ordinate (T_{Max}). The data fits were obtained by linear transformation using the homogeneous matrix system method, followed by determination of the constants by reduction to row echelon form. The resultant equations are given in Table 5 and the calculated data (solid lines) and extrapolations (dotted lines) are shown in Figure 7. The R^2 values for these equations were in the range of 0.90–0.98, which confirms the linear dependencies of the correlations.

Table 5. Generic equations for prediction of maximal curing temperature for selected Ms values and maximal temperatures to achieve 45 MPa compressive strength in 28 days for different slag contents.

Slag Content (wt%)	Generic Equation
20	Equation (7) $(-3.7272 \times Ms^2) + (-0.0788 \times Ms \times T_{Max}) + (-0.0131 \times T_{Max}^2) + Ms + T_{Max} + 1 = 0$
30	Equation (8) $(-10.3791 \times Ms^2) + (0.2491 \times Ms \times T_{Max}) + (-0.0142 \times T_{Max}^2) + Ms + T_{Max} + 1 = 0$
40	Equation (9) $(-2.6901 \times Ms^2) + (-0.1371 \times Ms \times T_{Max}) + (-0.0123 \times T_{Max}^2) + Ms + T_{Max} + 1 = 0$

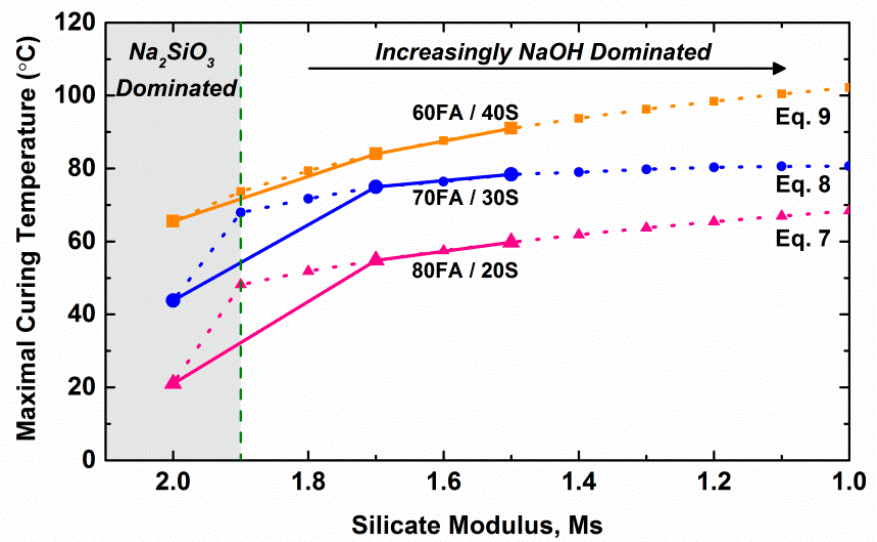

Figure 7. Data calculated from Figure 6 (solid lines) and values extrapolated using Equations (7)–(9) (dotted lines) for selected Ms values and slag contents (alkaline activator/SCM mass ratio = 0.5, water/binder ratio = 0.3).

Examination of Figure 7 demonstrates that the T_{Max} increases with decreasing Ms value for all samples, irrespective of the slag content. There is a sudden increase in the T_{Max} with slight changes in the Ms value from 2.0 to 1.7, followed by a gradual increase in T_{Max} with further reduction of Ms to 1.0. The data indicate that there are two regimes that are dominated by the two alkaline activators. At Ms = 2.0 to 1.9, there is a rapid increase in the T_{Max} with decreasing Ms value; at Ms = 1.9 to 1.0, the increase is more gradual. The positive slopes of the curves for these two regimes indicate that decreasing the Ms value allows curing at a higher temperature, thus allowing faster setting and greater user friendliness although at the expense of lower compressive strengths. All of these effects are more pronounced as the slag content increases, with the exception of the highest slag content at Ms = 2.0, which does not indicate a strong change in slope between the two regimes.

3.4. Relationship between 1-Day and 28-Day Compressive Strength

Figure 8A–F shows the correlation between the ratio of the 1-day and 28-day compressive strengths (σ_1/σ_{28}) as a function of curing temperature, Ms value, and slag content. The temperature at which the two strengths equalise at high temperatures is shown by the horizontal dashed lines, which are approached by the extrapolations of the experimental data. It can be seen that σ_1/σ_{28} increases linearly with curing temperature and that the rates (slopes) are nearly identical. It is clear that the geopolymer mortars cured at 60 °C achieved nearly maximal compressive strengths within 24 h of curing, so there is only a modest advantage to be gained from heat curing at temperatures >60 °C for the lower slag contents. It also can be seen that this compositional effect decreases with increasing Ms value. Finally, all of the extrapolations converge at a curing temperature of ~65 °C, which suggests that

heat curing for the purpose of rapid strength development in 24 h, regardless of Ms value and slag content, would be optimised at this curing temperature. Since the maximal curing temperature in these data is dictated by the slag content of 10 wt%, the slight effect of Ms value can be seen through the shift in the intersections of the extrapolations and the σ_1/σ_{28} = 1.0 line (T_{Max}):

- Ms = 2.0: T_{Max} = 65 °C
- Ms = 1.7: T_{Max} = 66 °C
- Ms = 1.5: T_{Max} = 68 °C

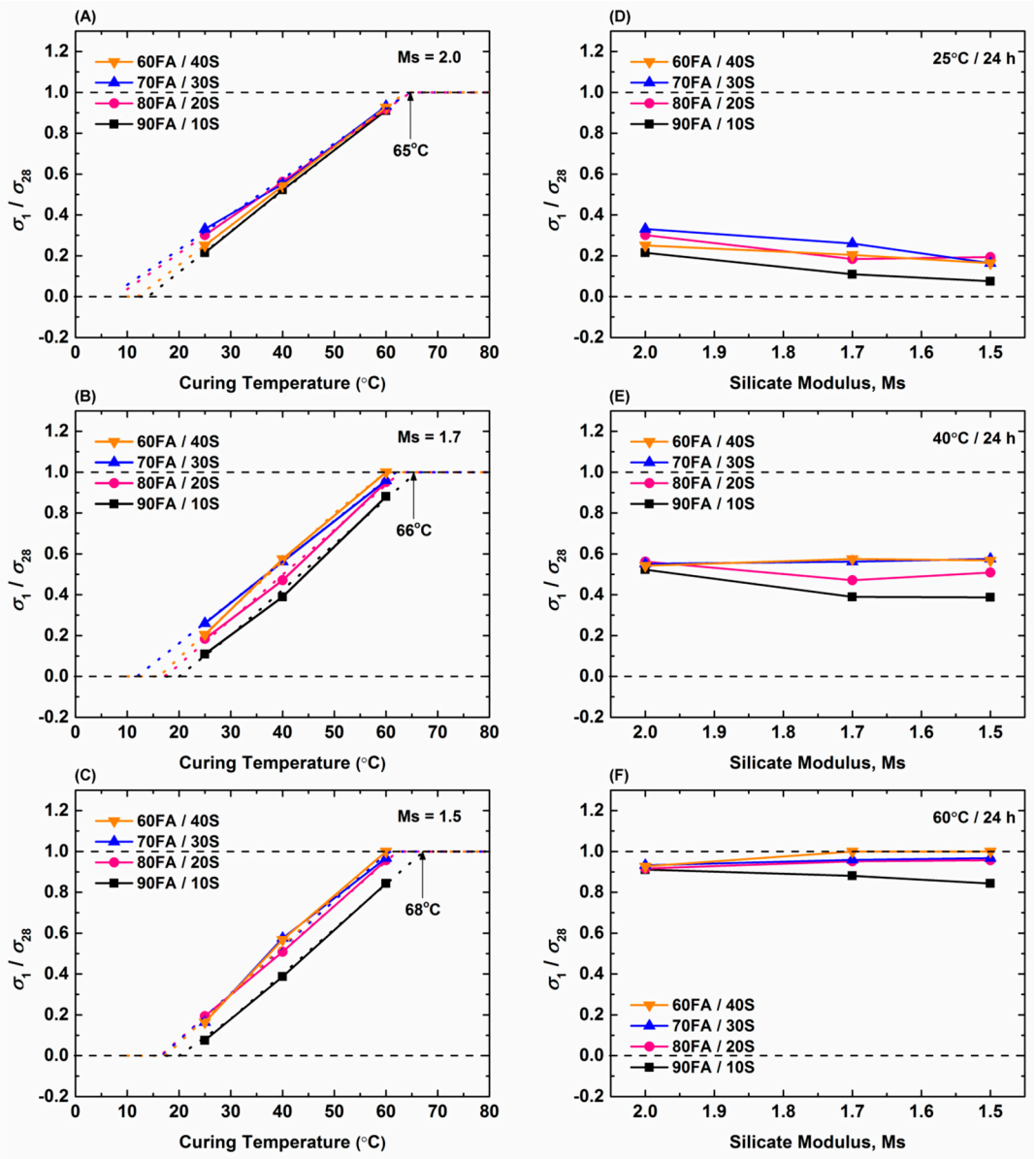

Figure 8. Ratio of 1-day to 28-day compressive strengths as a function of curing temperature, Ms value, and slag content. (**A**) Ms 2.0, (**B**) Ms 1.7, (**C**) Ms 1.5, (**D**) Cured for 25 °C/24 h, (**E**) Cured for 40 °C/24 h, (**F**) Cured for 60 °C/24 h.

In the other direction, the data in Figure 8A–C for lower temperatures show that, at 10°C, the extrapolation in σ_1/σ_{28} essentially trends to negative values for the geopolymer mortars. This suggests that geopolymer mortars with the corresponding compositions will not set within 24 h of curing under such cooling conditions.

In summary, Figure 8D–F indicates that the parameters that affect σ_1/σ_{28} can be ranked in the following order:

Curing Temperature >> Slag content > Ms Value

Figure 8D–F correlates σ_1/σ_{28} with the Ms value and show only a minimal influence, which appears to be a slight decrease in σ_1/σ_{28} with decreasing Ms value, with this effect more apparent for the lower slag contents. The principal effect derives from curing temperature, which shows the expected trend of increasing curing temperature accelerating the setting. The effect of composition is more prominent with decreasing Ms value.

The data in Figure 8A–C can be used in conjunction with those in Figure 6A–C to predict the 1-day compressive strength. That is, Figure 8A–C can be used to project a 28-day compressive strength at some particular curing temperature. The latter can be used in Figure 8A–C to project σ_1/σ_{28}, thereby allowing prediction of the 1-day strength at that curing temperature. Conversely, the data in Figure 8A–C can be used to project the 28-day compressive strength from testing after only 24 h. That is, at the curing temperature selected, compressive strength testing at 24 h for a particular composition would leave the 28-day compressive strength as the only unknown. This perhaps is the most applicable use of these data (Figure 8A–C) because they are nearly independent of Ms value and slag content.

4. Summary

In consideration of the data in the present work and those of comparable studies [15,16], Figure 9 is a schematic diagram of the generic strength development of geopolymer mortars as a function of ageing time, curing temperature, Ms value, and slag content.

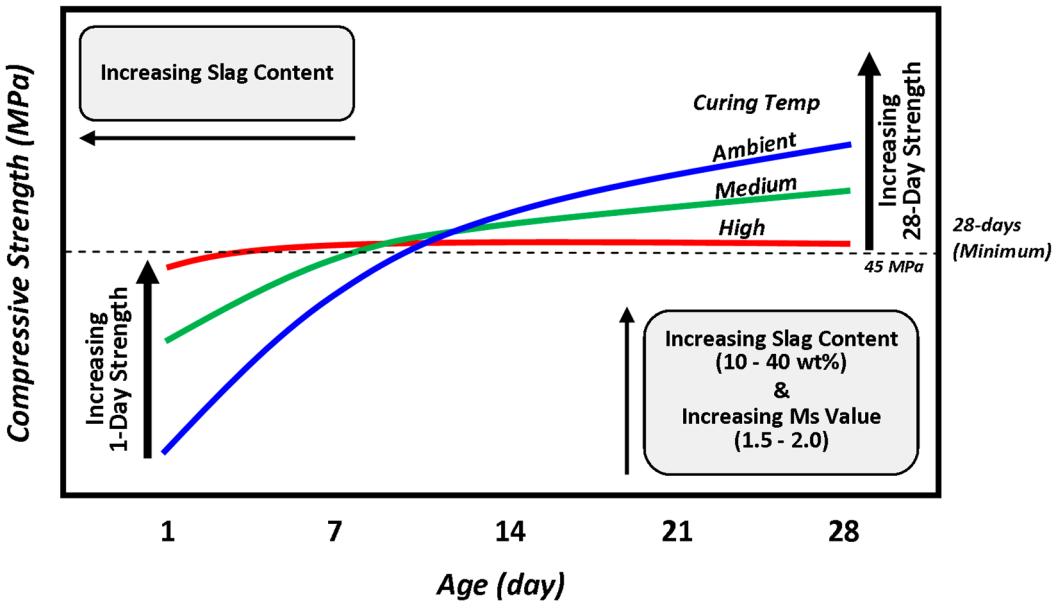

Figure 9. Schematic diagram showing the effect of curing temperature and slag content on strength development of geopolymer mortar.

The following conclusions can be drawn from this schematic:

- The 28-day compressive strength increases with decreasing curing temperature.
- The rate of strength development also increases with decreasing curing temperature.
- Conversely, the 1-day compressive strength increases with increasing curing temperature.
- The curing time required to reach the minimal 28-day strength requirement (45 MPa) increases with decreasing curing temperature.

- Increasing slag content decreases the curing time required to reach the minimal 28-day strength requirement (45 MPa).
- Increasing slag content increases the compressive strength at all time points.
- Decreasing Ms value increases the compressive strength at all time points except at 1 day.
- Maximisation of the compressive strengths can be achieved using the following relatively parametric values as shown in Table 6.

Table 6. Comparative experimental variables enabling maximisation of compressive strengths.

Compressive Strength	Priority Consideration	Curing Temperature	Ms Value	Slag Content
1 Day	Setting	High	Low	Low
28 Days	Strength	Low	Low	High

Beyond these data, the effects of the composition and temperature on the development of the compressive strength fall into two reaction mechanism regimes:

- Compositional Regimes: $\leq$30 wt% slag—Slow mechanism >30 wt% slag—Fast mechanism
- Temperature Regimes: 20 , 40 °C—Slow mechanism 60 °C—Fast mechanism

Further, the influence of the composition and curing temperature on the decremental 28-day compressive strength factor (the strength at an elevated curing temperature relative to that at ambient) fall into two reaction mechanism regimes:

- Compositional Regimes: Low slag content—No effect of Ms value High slag content/Ms = 2.0—Curing Temperature > Slag Content > Ms Value High slag content/Ms = 1.7, 1.5—Slag Content > Curing Temperature > Ms Value
- Temperature Regimes: Unclear regimes

The effects of the composition and curing temperature on the 28-day compressive strength also fall into two regimes:

- Compositional Regimes: $\leq$30 wt% slag—Slow mechanism >30 wt% slag—Fast mechanism
- Temperature Regimes: No differentiable regimes

The effects of composition and curing temperature on the 28-day compressive strength are clarified by the data in Figure 6A–C:

- Cold-Weather Casting: The compressive strength is greater than that at ambient and the differential increases with increasing slag content.
- Heat Curing: The compressive strength is lower than that at ambient and the differential increases with increasing slag content.

The effects of the slag content and Ms value on the maximal curing temperature (T_{Max}) also fall into two regimes:

- Compositional Regimes: Ms $\leq$ 1.9—NaOH dominated—Increasing Ms value slightly decreases T_{Max} Ms > 1.9—Na_2SiO_3 dominated—Increasing Ms value greatly decreases T_{Max}
- Temperature Regimes: Not applicable

In consideration of the data in Figure 8A–C. Figure 10 is a schematic of the ratio of the 1-day and 28-day compressive strengths (σ_1/σ_{28}) as a function of curing temperature, Ms value, and slag content.

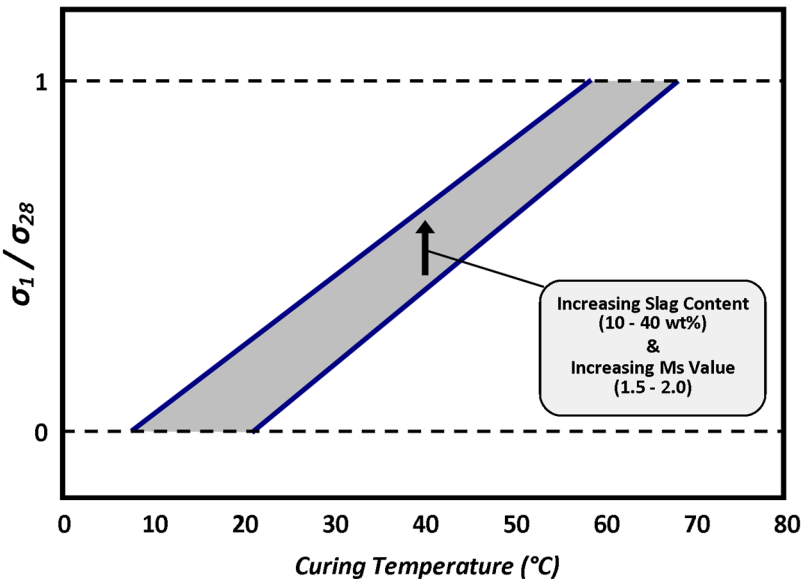

Figure 10. Schematic diagram summarising the effect of curing temperature, Ms value, and slag content on σ_1/σ_{28}.

The following conclusions can be drawn from this schematic:

- The σ_1/σ_{28} increases with increasing curing temperature.
- The slope of this relation is nearly independent of Ms value and slag content.
- The convergence of the extrapolations indicates that the maximal curing temperature (T_{Max}), beyond which no advantage is to be gained, is ~65 °C.
- Increasing the slag content appears to give only a slight increase in the σ_1/σ_{28} value for the same curing temperature.
- Increasing the Ms value gives only a slight increase in the σ_1/σ_{28} value for the same curing temperature.

Beyond these data, the effects of the composition and temperature on the σ_1/σ_{28} ratio are:

- For cold-weather casting conditions, the 28-day compressive strengths that can be achieved are equivalent to those at ambient temperature, although setting will be delayed.
- The effects of the experimental value can be ranked:

Curing Temperature >> Slag content > Ms Value

The data in Figure 6A–C and Figure 8A–C, which give the 28-day compressive strength and σ_1/σ_{28}, respectively, as a function of curing temperature, can be used jointly to predict the 28-day compressive following testing after only 1 day. It is notable that the data provided are for geopolymers with a water/binder ratio of 0.3. For mixes with excessive water contents, these correlations may not be valid since higher water contents would be likely to increase the workability, setting time, and gel formation. Further, heat curing also would be likely to increase the net loss of water, thereby enhancing cracking from shrinkage and pore generation from water evaporation. All of these would be expected to reduce the rate and extent of compressive strength development. Conversely, for mixes with insufficient water contents, the strength development would be impacted negatively owing to the reduced extents of solubility of the activators.

Author Contributions: Data curation, S.U. and C.F.; formal analysis, S.U., P.K., A.R. and C.C.S.; funding acquisition, A.C.; investigation, P.K.; resources, P.K., A.C. and C.C.S.; supervision, P.K., A.R., A.C. and C.C.S.; writing—original draft, S.U.; writing—review and editing, S.U., P.K., A.C. and C.C.S. All authors have read and agreed to the published version of the manuscript.

Funding: This research work is partially funded by the Cooperative Research Centre (CRC) for Low Carbon Living, an Australian Government initiative (grant number RP1020).

Institutional Review Board Statement: Not applicable.

Informed Consent Statement: Not applicable.

Data Availability Statement: Not applicable.

Acknowledgments: The lead author also would like to thank UNSW Sydney for the University International Postgraduate Award that supported this work. The authors also are grateful for the subsidised facilities for characterisation provided by the Mark Wainwright Analytical Centre, UNSW Sydney.

Conflicts of Interest: There are no conflicts of interest to declare.

References

1. Turner, L.K.; Collins, F.G. Carbon Dioxide Equivalent (CO2-e) Emissions: A Comparison between Geopolymer and OPC Cement Concrete. *Constr. Build. Mater.* **2013**, *43*, 125–130. [CrossRef]
2. Provis, J.L.; van Deventer, J.S.J. (Eds.) *Geopolymers: Structure, Processing, Properties and Industrial Applications*; Woodhead Publishing: Oxford, UK, 2009.
3. Ukritnukun, S.; Koshy, P.; Rawal, A.; Castel, A.; Sorrell, C.C. Predictive Model of Setting Times and Compressive Strengths for Low-Alkali, Ambient-Cured, Fly Ash/Slag-Based Geopolymers. *Minerals* **2020**, *10*, 920. [CrossRef]
4. Atis, C.D.; Görur, E.B.; Karahan, O.; Bilim, C.; Ilkentapar, S.; Luga, E. Very High Strength (120 MPa) Class F Fly Ash Geopolymer Mortar Activated at Different NaOH Amount, Heat Curing Temperature and Heat Curing Duration. *Constr. Build. Mater.* **2015**, *96*, 673–678. [CrossRef]
5. Wallah, S.; Rangan, B.V. *Low-Calcium Fly Ash-Based Geopolymer Concrete: Long-Term Properties*; Research Report GC2; Faculty of Engineering, Curtin University of Technology: Perth, Australia, 2006.
6. Fernández-Jiménez, A.; Garcia-Lodeiro, I.; Palomo, A. Durability of Alkali-Activated Fly Ash Cementitious Materials. *J. Mater. Sci.* **2007**, *42*, 3055–3065. [CrossRef]
7. Sumajouw, D.M.J.; Hardjito, D.; Wallah, S.E.; Rangan, B.V. Fly Ash-Based Geopolymer Concrete: Study of Slender Reinforced Columns. *J. Mater. Sci.* **2007**, *42*, 3124–3130. [CrossRef]
8. Castel, A.; Foster, S.J. Bond Strength between Blended Slag and Class F Fly Ash Geopolymer Concrete with Steel Reinforcement. *Cem. Concr. Res.* **2015**, *72*, 48–53. [CrossRef]
9. Sarker, P.K.; Haque, R.; Ramgolam, K.V. Fracture Behaviour of Heat Cured Fly Ash Based Geopolymer Concrete. *Mater. Des.* **2013**, *44*, 580–586. [CrossRef]
10. Castel, A.; Foster, S.J.; Ng, T.; Sanjayan, J.G.; Gilbert, R.I. Creep and Frying Shrinkage of a Blended Slag and Low Calcium Fly Ash Geopolymer Concrete. *Mater. Struct.* **2016**, *49*, 1619–1628. [CrossRef]
11. Mikuni, A.; Komatsu, R.; Ikeda, K. Dissolution Properties of Some Fly Ash Fillers Applying to Geopolymeric Materials in Alkali Solution. *J. Mater. Sci.* **2007**, *42*, 2953–2957. [CrossRef]
12. Kumar, S.; Kumar, R.; Mehrotra, S. Influence of Granulated Blast Furnace Slag on the Reaction, Structure and Properties of Fly Ash Based geopolymer. *J. Mater. Sci.* **2010**, *45*, 607–615. [CrossRef]
13. Zhang, Z.; Provis, J.L.; Reid, A.; Wang, H. Geopolymer Foam Concrete: An Emerging Material for Sustainable Construction. *Constr. Build. Mater.* **2014**, *56*, 113–127. [CrossRef]
14. Panagiotopoulou, C.; Kontori, E.; Perraki, T.; Kakali, G. Dissolution of Aluminosilicate Minerals and By-Products in Alkaline Media. *J. Mater. Sci.* **2007**, *42*, 2967–2973. [CrossRef]
15. Rovnaník, P. Effect of Curing Temperature on the Development of Hard Structure of Metakaolin-Based Geopolymer. *Constr. Build. Mater.* **2010**, *24*, 1176–1183. [CrossRef]
16. Chindaprasirt, P.; Chareerat, T.; Hatanaka, S.; Cao, T. High-Strength Geopolymer Using Fine High-Calcium Fly Ash. *J. Mater. Civ. Eng.* **2011**, *23*, 264–270. [CrossRef]
17. Noushini, A.; Babaee, M.; Castel, A. Suitability of Heat-Cured Low-Calcium Fly Ash-Based Geopolymer Concrete for Precast Applications. *Mag. Concr. Res.* **2016**, *68*, 163–177. [CrossRef]
18. Chindaprasirt, P.; Jaturapitakkul, C.; Chalee, W.; Rattanasak, U. Comparative Study on the Characteristics of Fly Ash and Bottom Ash Geopolymers. *Waste Manag.* **2009**, *29*, 539–543. [CrossRef]
19. Patankar, S.V.; Ghugal, Y.M.; Jamkar, S.S. Effect of Concentration of Sodium Hydroxide and Degree of Heat Curing on Fly Ash-Based Geopolymer Mortar. *Indian J. Mater. Sci.* **2014**, *2014*, 938789. [CrossRef]
20. Chi, M.C.; Liu, Y.C. Effects of Fly Ash/Slag Ratio and Liquid/Binder Ratio on Strength of Alkali-Activated Fly Ash/Slag Mortars. In *Applied Mechanics and Materials*; Trans Tech Publications: Stafa-Zurich, Switzerland, 2013; pp. 50–54.
21. Rao, G.M.; Rao, T.D.G. Final Setting Time and Compressive Strength of Fly Ash and GGBS-Based Geopolymer Paste and Mortar. *Arab. J. Sci. Eng.* **2015**, *40*, 3067–3074.

22. Phoo-ngernkham, T.; Sata, V.; Hanjitsuwan, S.; Ridtirud, C.; Hatanaka, S.; Chindaprasirt, P. High Calcium Fly Ash Geopolymer Mortar Containing Portland Cement for Use as Repair Material. *Constr. Build. Mater.* **2015**, *98*, 482–488. [CrossRef]
23. Temuujin, J.; van Riessen, A.; MacKenzie, K.J.D. Preparation and Characterisation of Fly Ash Based Geopolymer Mortars. *Constr. Build. Mater.* **2010**, *24*, 1906–1910. [CrossRef]
24. Pangdaeng, S.; Phoo-ngernkham, T.; Sata, V.; Chindaprasirt, P. Influence of Curing Conditions on Properties of High Calcium Fly Ash Geopolymer Containing Portland Cement as Additive. *Mater. Des.* **2014**, *53*, 269–274. [CrossRef]
25. Sata, V.; Sathonsaowaphak, A.; Chindaprasirt, P. Resistance of Lignite Bottom Ash Geopolymer Mortar to Sulfate and Sulfuric Acid Attack. *Cem. Concr. Compos.* **2012**, *34*, 700–708. [CrossRef]
26. Adam, A.A. Horianto The Effect of Temperature and Duration of Curing on the Strength of Fly Ash Based Geopolymer Mortar. *Procedia Eng.* **2014**, *95*, 410–414. [CrossRef]
27. Rattanasak, U.; Chindaprasirt, P. Influence of NaOH Solution on the Synthesis of Fly Ash Geopolymer. *Miner. Eng.* **2009**, *22*, 1073–1078. [CrossRef]
28. Chindaprasirt, P.; Chareerat, T.; Sirivivatnanon, V. Workability and Strength of Coarse High Calcium Fly Ash Geopolymer. *Cem. Concr. Compos.* **2007**, *29*, 224–229. [CrossRef]
29. Qu, F.; Li, W.; Tao, Z.; Castel, A.; Wang, K. High Temperature Resistance of Fly Ash/GGBFS-Based Geopolymer Mortar with Load-Induced Damage. *Mater. Struct.* **2020**, *53*, 111. [CrossRef]
30. Kurklu, G. The Effect of High Temperature on the Design of Blast Furnace Slag and Coarse Fly Ash-Based Geopolymer Mortar. *Compos. Part B Eng.* **2016**, *92*, 9–18. [CrossRef]
31. Manesh, B.S.; Madhukar, R.W.; Subhash, V.P. Effect of Duration and Temperature of Curing on Compressive Strength of Geopolymer Concrete. *Int. J. Eng. Innov. Technol.* **2012**, *1*, 152–155.
32. Zhuang, H.; Li, L.; Wang, Q.; Sarker, P.K.; Shi, X. Deterioration of Ambient-Cured and Heat-Cured Fly Ash Geopolymer Concrete by High Temperature Exposure and Prediction of its Residual Compressive Strength. *Constr. Build. Mater.* **2020**, *262*, 120924. [CrossRef]
33. Junaid, M.T.; Kayali, O.; Khennane, A. Response of Alkali Activated Low Calcium Fly-Ash Based Geopolymer Concrete under Compressive Load at Elevated Temperatrures. *Mater. Struct.* **2017**, *50*, 50. [CrossRef]
34. Shoaei, P.; Musaeei, H.R.; Mirlohi, F.; Zamanabadi, S.N.; Ameri, F.; Bahrami, N. Waste Ceramic Powder-Based Geopolymer Mortars: Effect of Curing Temperature and Alkaline Solution-to-Binder Ratio. *Constr. Build. Mater.* **2019**, *227*, 116686. [CrossRef]
35. Assi, L.N.; Deaver, E.; ElBatanouny, M.K.; Ziehl, P. Investigation of Early Compressive Strength of Fly Ash-Based Geopolymer Concrete. *Constr. Build. Mater.* **2016**, *112*, 807–815. [CrossRef]
36. Karthik, A.; Sudalaimani, K.; Kumar, C.T.V. Investigation on Mechanical Properties of Fly Ash-Ground Granulated Blast Furnace Slag Based Self Curing Bio-Geopolymer Concrete. *Constr. Build. Mater.* **2017**, *149*, 338–349. [CrossRef]
37. *Supplementary Cementitious Materials Part1: Fly Ash*; AS/NZS 3582.1; Standards Australia Limited: Sydney, Australia, 2016.
38. *Supplementary Cementitious Materials Part 2: Slag—Ground Granulated Blast Furnace*; AS/NZS 3582.2; Standards Australia Limited: Sydney, Australia, 2016.
39. *Standard Test Method for Relative Density (Specific Gravity) and Absorption of Fine Aggregate*; ASTM C128-15 A. C128-15; ASTM International: West Conshohocken, PA, USA, 2015.
40. Kosmatka, S.H.; Kerkhoff, B.; Panarese, W.C. *Design and Control of Concrete Mixtures*; Portland Cement Association: Skokie, IL, USA, 2008.
41. Provis, J.L.; Yong, C.Z.; Duxson, P.; van Deventer, J.S.J. Correlating mechanical and thermal properties of sodium silicate-fly ash geopolymers. *Physicochem. Eng. Asp.* **2009**, *336*, 57–63. [CrossRef]
42. Xie, Z.; Xi, Y. Hardening mechanisms of an alkaline-activated class F fly ash. *Cem. Concr. Res.* **2001**, *31*, 1245–1249. [CrossRef]
43. Kong, D.Y.; Sanjayan, J.; Sagoe-Crentsil, K. Factors Affecting the Performance of Metakaolin Geopolymers Exposed to Elevated Temperatures. *J. Mater. Sci.* **2008**, *43*, 824–831. [CrossRef]
44. Soleimani, M.; Naghizadeh, R.; Mirhabibi, A.; Golestanifard, F. Effect of Calcination Temperature of the Kaolin and Molar Na2O/SiO2 Activator Ratio on Physical and Microstructural Properties of Metakaolin Based Geopolymers. *Iran. J. Mater. Sci. Eng.* **2012**, *9*, 43–51.
45. Thakur, R.N.; Ghosh, S. Effect of Mix Composition on Compressive Strength and Microstructure of Fly Ash Based Geopolymer Composites. *Int. J. Appl. Eng. Res.* **2009**, *4*, 68–74.
46. *Standard Test Method for Compressive Strength of Hydraulic Cement Mortars (Using 2-in. or [50-mm] Cube Specimens)*; ASTM C109M-13; ASTM International: West Conshohocken, PA, USA, 2013.
47. *General Purpose and Blended Cements*; AS 3972-2010; Standards Australia Limited: Sydney, Australia, 2010.
48. Speight, J.G. Chapter Four—Properties of Inorganic Compounds. In *Environmental Inorganic Chemistry for Engineers*; Butterworth-Heinemann (Elsevier): Amsterdam, The Netherlands, 2017; pp. 171–229.
49. Temuujin, J.; Williams, R.P.; van Riessen, A. Effect of Mechanical Activation of Fly Ash on the Properties of Geopolymer Cured at Ambient Temperature. *J. Mater. Process. Technol.* **2009**, *209*, 5276–5280. [CrossRef]